RSC Advances

PAPER

View Article Online
View Journal | View Issue

Cite this: *RSC Adv.*, 2025, **15**, 33224

In situ growth of luminescent lanthanide coordination nanoparticles inside living plants

Xinnan Wang, Chunyu Zhao, Qi Wang, Xiaowen Wang, Tao Chen, Xinyue Yang, Keyi Guo and Qi Zhou *

Lanthanide coordination nanoparticles have drawn considerable attention owing to their outstanding luminescence properties. However, biosynthesis of lanthanide coordination nanoparticles is a relatively new and poorly explored area. Plants possess complex passive fluid transport systems and are potential green nanofactories for the synthesis of nanomaterials. In this study, luminescent lanthanide coordination nanoparticles with various morphologies were synthesized from various living plants. The two-step process involved incubating plant clippings or intact plants in *p*-phthalic acid (PTA) solution, followed by washing and subsequent incubation in lanthanide ion (Eu^{3+} and Tb^{3+}) solution. Different types of plants and lanthanide ions led to the formation of lanthanide coordination nanoparticles of different shapes and sizes. Specifically, the Eu/PTA and Tb/PTA coordination nanoparticles inside *shamrock* and *epipremnum aureum* revealed spherical, rod-shaped, octahedral, cubic, and rectangular crystals with sizes in the nanometer and micrometer ranges. Moreover, luminescent *shamrocks* with red, green, and even yellow emissions were obtained using Eu^{3+}, Tb^{3+}, and a mixture. Finally, the intact *shamrocks* with luminescent Eu/PTA and Tb/PTA coordination nanoparticles were used for the *in situ* detection of Cu^{2+} in water. The integration of functional lanthanide coordination nanoparticles into living plants is a promising innovation in nanobionics that could open the door to advanced sensors and other applications.

Received 19th June 2025
Accepted 6th September 2025

DOI: 10.1039/d5ra04355g

rsc.li/rsc-advances

Introduction

Lanthanide coordination nanoparticles (Ln-CNs) are a subclass of lanthanide-based materials formed by bridging organic ligands and lanthanide ions.[1–3] They have been applied in the fields of drug delivery, catalysis, bioimaging, and sensing, owing to their outstanding luminescent properties and adjustable structures.[4–11] Accordingly, the synthesis of high-performance Ln-CNs is the cornerstone of various potential applications. However, Ln-CNs are typically synthesized by chemical coprecipitation, thermal decomposition, and hydrothermal/solvothermal methods. These methods involve expensive techniques, inefficient energy consumption, and environmental risks. In recent years, the fabrication of Ln-CNs has become increasingly cost-effective and environmentally benign with the rapid development of nanotechnology. Consequently, green synthesis technologies mediated by biological systems (such as bacteria, fungi, algae, and plants) are growing rapidly because of the wide range of raw material sources, their low cost, and mild reaction conditions.[12–15]

However, the biosynthesis of Ln-CNs-particularly for *in situ* growth within living plants-is a relatively new and largely unexplored area.[16,17] Plants have complex vascular networks capable of internalizing foreign metal ions and organic molecules from the environment through cohesive and adhesive forces.[18–20] The Ln-CN precursors are able to be absorbed by the plants and accumulate around biomolecules, allowing the Ln-CNs to grow. Moreover, the presence of biomolecules and bioentities can accelerate Ln-CN growth considerably.[21,22] Therefore, living plants are potential green nanofactories for synthesizing nanomaterials such as Ln-CNs. For example, Liang *et al.* reported the synthesis of $Eu_2(BDC)_3$, and $Tb_2(BDC)_3$ coordination nanoparticles inside reeds, lilies, lotuses, and *syngonium podophyllum*.[23] The integration of functional nanomaterials and living plants is a promising innovation in bioaugmentation and nanobionics, which could open the door to advanced sensors and other applications. However, the process of *in situ* Ln-CN growth within living plants remains largely unexplored. In particular, the physicochemical properties of in-vivo-synthesized Ln-CNs are not yet fully understood.

In this study, we demonstrated that luminescent Ln-CNs of varying shapes and sizes could be synthesized inside plant clippings and in intact plants (Fig. 1). Plants were added to an aqueous solution of *p*-phthalic acid (PTA), washed, and subsequently added to a solution of lanthanide ions (Tb^{3+} and Eu^{3+}). Scanning electron microscopy (SEM) combined with elemental mapping was used to confirm the formation of Ln-CNs.

School of Life Sciences, Zhengzhou University, Zhengzhou 450001, China. E-mail: qzhou@zzu.edu.cn

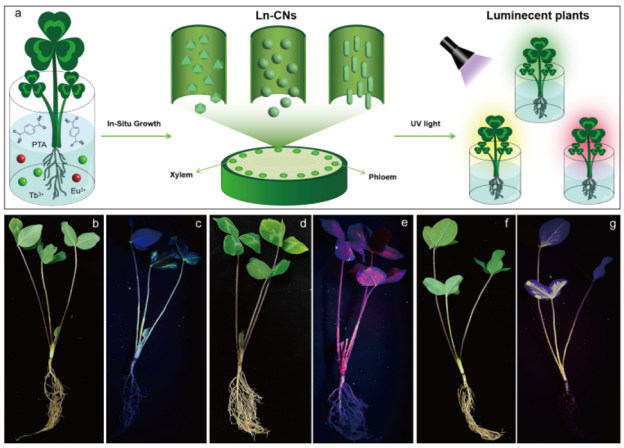

Fig. 1 (a) Illustration of Ln-CNs formation inside of plants. Camera images of intact *shamrocks* after Ln-CNs growth under daylight (b, d and f) and 254 nm UV light (c, e and g). (b) Tb/PTA coordination nanoparticles were grown. (d) Eu/PTA coordination nanoparticles were grown. (f) Eu/Tb/PTA coordination nanoparticles (Eu : Tb = 1 : 5) were grown.

Different plant species and lanthanide ions can lead to the formation of Ln-CNs with various morphologies. Specifically, the Eu/PTA and Tb/PTA coordination nanoparticles inside *shamrock* and *epipremnum aureum* exhibited distinct shapes and sizes compared to those in previous reports.[17,23] Moreover, using Eu^{3+}, Tb^{3+}, and their mixture, we could obtain luminescent *shamrocks* with red, green, and even yellow emissions. Finally, the intact *shamrocks* with Eu/PTA and Tb/PTA coordination nanoparticles grown within were used as luminescence "turn-off" probes for real-time monitoring of Cu^{2+} in water.

Experimental

Materials

Europium chloride hexahydrate ($EuCl_3 \cdot 6H_2O$, 99.9%), terbium chloride hexahydrate ($TbCl_3 \cdot 6H_2O$, 99.9%), *p*-phthalic acid (PTA, 99%), and copric chloride dihydrate ($CuCl_2 \cdot 2H_2O$, 99.9%) were purchased from Shanghai Macklin Biochemical Co., Ltd and used as received.

Plant growth

Intact *shamrock* and *humulus scandens* were obtained from shrubbery at the Zhengzhou University campus (Zhengzhou, Henan, China). *Epipremnum aureum* was purchased from a flower market. The plants were freshly obtained and cultivated in a light incubator (Yanghui MGC-500C). The plant clippings were prepared from intact plants. The basic experimental parameters were as follows: temperature: 25 °C, light source: 6500 K white light, photoperiod: 14 h daily, air humidity: 60%.

Ln-CNs formation in plants

PTA (166 mg), terbium chloride hexahydrate (283 mg), and europium chloride hexahydrate (276 mg) were separately dissolved in glass beakers containing 50 mL ultrapure water. The roots of an intact plant or the base of the plant clippings were first immersed in a glass beaker containing PTA aqueous solution (20 mM, 50 mL) for 12 h, followed by gentle washing with running tap water (at room temperature) for 5 min and subsequent culturing in an aqueous solution (50 mL) containing 20 mM lanthanide ions (Tb^{3+} and Eu^{3+}) for another 12 h. Subsequently, the Ln-CNs were grown within the plants.

In situ detection of Cu^{2+} in water

The intact *shamrocks* with Eu/PTA and Tb/PTA coordination nanoparticles grown within were washed gently with tap water and incubated with 50 mM Cu^{2+} solution. After 12 and 24 h, the *shamrocks* were separately imaged under a UV lamp at 254 nm.

Characterization

Plant stem samples were freeze-dried and coated with a thin layer of gold. Morphological analysis was recorded on field-emission scanning electron microscopy (Hitachi, SU8010) at an accelerating voltage of 3 kV. Energy dispersive X-ray spectroscopy (EDS) studies were also conducted in parallel to confirm the formation of the Ln-CNs.

Results and discussion

PTA is a common ligand of lanthanide ions, which can sensitize the luminescence of Eu^{3+} and Tb^{3+}.[24–26] PTA and lanthanide ions were able to rapidly and readily form flakes Ln-CNs in water, showing red and green luminescence under 254 nm UV light (Fig. S1). According to previous reports,[17,23] for Ln-CNs that form rapidly, the plants should be successively immersed in a single metal salt solution and organic ligand solution. Furthermore, the organic ligands would be better for the first incubation stage because the lanthanide ions are small enough to move through the pores of the Ln-CNs and thus would not be hindered by the Ln-CNs growth.[23] Consequently, a two-step Ln-CNs synthesis process was used in our experiments. In the first step, the plants were immersed in a PTA solution, followed by washing and subsequent incubation in a lanthanide ions solution. The PTA and lanthanide ions were absorbed by the plants and accumulated around their biomolecules, allowing the Ln-CNs to grow. The Ln-CNs formed using various lanthanide ions (Eu^{3+} and Tb^{3+}) were denoted as Eu/PTA, Tb/PTA, and Eu/Tb/PTA coordination nanoparticles, respectively.

Initial tests were conducted with plant clippings as trimming the plant at the stem allowed larger molecules to accumulate through cohesive and adhesive forces.[23] *Shamrock* is a common herbaceous plant with a wide distribution and strong adaptability, which is cultivated worldwide. After freshly obtaining the intact *shamrock* from shrubbery at our campus, the clippings were prepared and incubated with PTA solution overnight. The green and red luminescence were observed in the stems after 4 h of incubation with Tb^{3+} and Eu^{3+} ions, respectively. Analyses of the cross-section of the stem under 254 nm UV light (Fig. S2) confirmed the formation of the luminescent compounds. As the incubation time of Eu^{3+} and Tb^{3+} increased, the luminescent coordination nanoparticles gradually formed

in the leaves (Fig. 2a and b), making the vasculature of *shamrock* clearly visible under UV light. Similar results were evident when using *epipremnum aureum* (Fig. 2c) and *humulus scandens* (Fig. 2d).

In order to further confirm the formation of Ln-CNs, the structures of luminescent compounds grown within the plants were examined using SEM. As illustrated in Fig. 2e and f, the morphology of the Eu/PTA coordination nanoparticles within the *shamrock* was a uniform sphere of approximately 30–70 μm size. It is worth noting that it was larger than reported Eu/PTA coordination nanoparticles,[23] possibly owing to the involvement of different plant biomolecules in the formation of the coordination nanoparticles. However, when changed to Tb^{3+} ions, the Tb/PTA coordination nanoparticles grown in the *shamrock* formed irregular nanoparticles (Fig. S3). Moreover, the SEM images revealed that the Tb/PTA coordination nanoparticles within the *epipremnum aureum* had regular nanorod crystals with an average diameter of approximately 200 nm (Fig. 2g and h). The rod-shaped Ln-CNs gathered like blooming flowers. By contrast, Fig. 2i and j showed that a heterogeneous mixture of Eu/PTA coordination nanoparticles, ranging in size from 500 nm to 2 μm, were grown within the *epipremnum aureum*. In addition to nanospheres, anisotropic Eu/PTA coordination nanoparticles—such as octahedral, cubic, and cuboid coordination nanoparticles—could be observed (marked by red arrows). EDS elemental analysis of the Ln-CNs is illustrated in Fig. S4. The existence of europium and terbium elements confirmed the formation of Eu/PTA and Tb/PTA coordination nanoparticles within the plant clippings.

The outstanding performance of plant clippings inspired us to synthesize Ln-CNs within intact plants through the mass flow of PTA and lanthanide ions into the roots, followed by transport through the xylem. Only in this manner could various applications be envisioned, such as living sensors. Although the uptake of the precursors and *in situ* growth of Eu/PTA and Tb/PTA coordination nanoparticles were hampered within intact *shamrocks* compared to the *shamrock* clippings, the *shamrocks* were still able to emit luminescence under 254 nm UV light (Fig. 3a and b). However, the Eu/PTA and Tb/PTA coordination nanoparticles grew only in specific segments of *shamrocks* owing to the asymmetries in the uptake and transport through the roots (Fig. 3c). Specifically, not all leaves exhibited the luminescent signature of Eu/PTA and Tb/PTA coordination nanoparticles (Fig. 3d and e).

SEM images revealed that the Eu/PTA and Tb/PTA coordination nanoparticles synthesized through root absorption were smaller than those transported through the stems. The morphology of the Tb/PTA coordination nanoparticles within the intact *shamrock* was a regular nanosphere of approximately 50 nm size, whereas the Eu/PTA coordination nanoparticles revealed spiny nanosphere crystals with an average diameter of approximately 150 nm. In addition, when PTA was changed to pyridine-2,6-dicarboxylic acid (another common sensitizer of lanthanide ions),[27,28] the luminescent *shamrocks* with red, green, and even yellow emissions can also be obtained (Fig. S5).

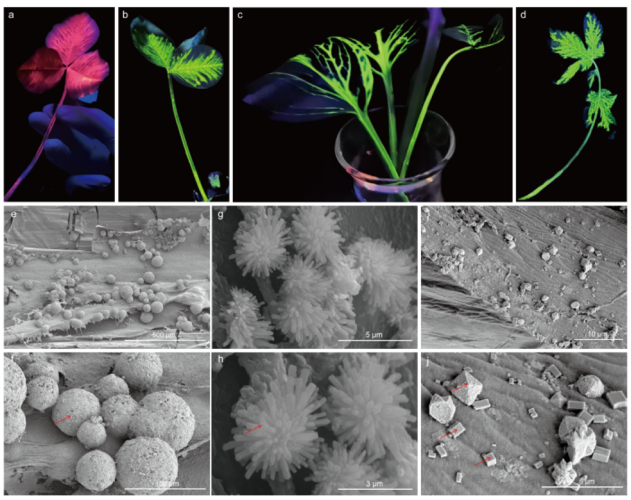

Fig. 2 Camera images of plant clippings with Ln-CNs growth under 254 nm UV light (a–d). (a) *Shamrock* with Eu/PTA coordination nanoparticles growth. (b) *Shamrock* with Tb/BDC coordination nanoparticles growth. (c) *Epipremnum aureum* with Tb/PTA coordination nanoparticles growth. (d) *Humulus scandens* with Tb/PTA coordination nanoparticles growth. (e–j) SEM images of longitudinal sections of plant stems with Ln-CNs growth within. (e and f) *Shamrock* with Eu/PTA coordination nanoparticles growth. (g and h) *Epipremnum aureum* with Tb/PTA coordination nanoparticles growth. (i and j) *Epipremnum aureum* with Eu/PTA coordination nanoparticles growth.

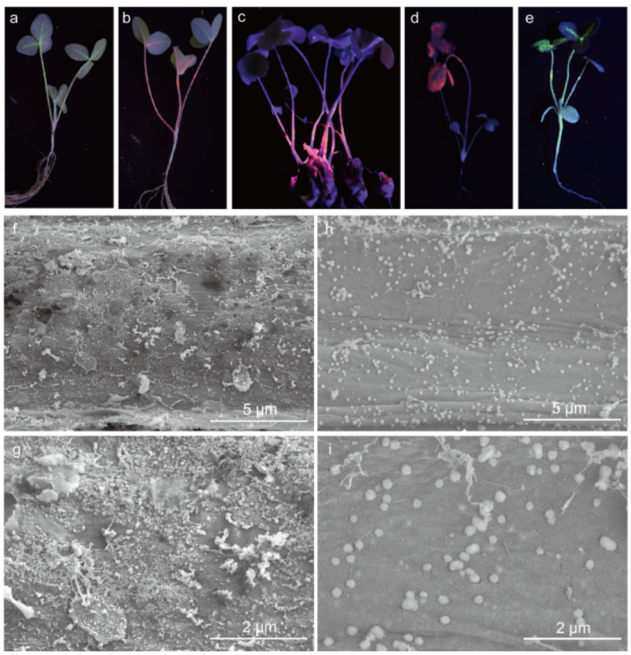

Fig. 3 Camera images of the intact *shamrocks* with Ln-CNs growth within under 254 nm UV light (a–e). (a and e) Tb/PTA coordination nanoparticles were grown. (b, c, and d) Eu/PTA coordination nanoparticles were grown. (f–i) SEM images of longitudinal sections of the intact *shamrocks* stems with Ln-CNs growth within. (f and g) Tb/PTA coordination nanoparticles were grown. (h and i) Eu/PTA coordination nanoparticles were grown.

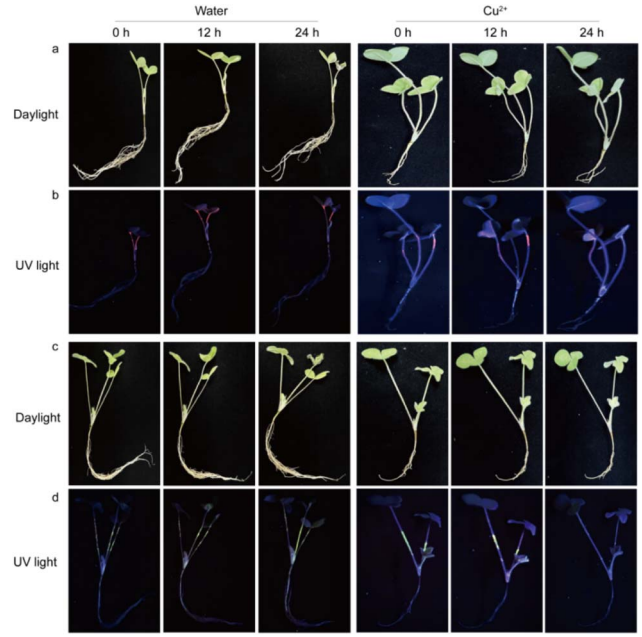

Fig. 4 Camera images of the intact *shamrocks* with Ln-CNs growth under daylight (a and c) and 254 nm UV light (b and d) conditions when cultivated in water or Cu^{2+} solution (50 mM). (a) Eu/PTA coordination nanoparticles were grown. (c) Tb/PTA coordination nanoparticles were grown.

Nanomaterials have been widely used in portable, sensitive, and high-throughput sensing platforms due to their unique physical and chemical properties.[29,30] It is a research hotspot to integrate functionalized nanoparticles into living plants to construct plant nanobionic sensors.[31,32] In addition, plants possess vast root network structure capable of automatically extracting samples from underground environment.[33] The natural circuitry consisting of roots, stems, and leaves enables rapid and efficient transport of various substances.[34] Environmental pollutants generally enter plants through their roots and leaves. Some pollutants will be gradually catabolized, while others will accumulate in plants.[35] These characteristics enable plants to be used as environmental sensors to indicate specific pollutants. For example, wong *et al.* reported the use of functionalized single walled carbon nanotubes to create nanobionic-plant-enabled sensors that detect nitroaromatics in real time *via* attenuation of near-infrared fluorescence in leaves of living spinach plants.[36] Similarly, lew *et al.* demonstrated the integration of DNA-wrapped single walled carbon nanotubes with living wild-type plants to engineer plant nanobionic sensors capable of real-time detection of arsenite in the belowground environment.[37]

Ln-CNs have been widely applied in chemical and biological sensing and detection through changes in luminescence.[38,39] Consequently, we tested whether our luminescent plants could be used as living sensors. According to previous reports,[17,23] plants can serve as self-powered preconcentrators *via* their passive fluid transport systems and accumulate various toxic metal ions and organic pollutants around the embedded Ln-CNs, resulting in relative changes in their luminescence intensity. Accordingly, the luminescent intact *shamrocks* with Eu/PTA coordination nanoparticles growth were incubated in a Cu^{2+} solution (50 mM) and water. As illustrated in Fig. 4a, after 24 h, all the *shamrocks* grew normally and exhibited no major changes in daylight. However, under UV light, there was no major difference in the luminescence of the *shamrocks* immersed in water, whereas the luminescence of the *shamrocks* immersed in the Cu^{2+} solution disappeared after 24 h (Fig. 4b). Similar performances were also observed when using the *shamrocks* with Tb/PTA coordination nanoparticles growth (Fig. 4c and d). These results suggest that the plant-Ln-CNs hybrid may serve as a tool for the *in situ* detection of small-molecule contaminants in hydroponic setups.

Conclusions

This study demonstrated that different Ln-CNs could be synthesized in a two-step process for both clipped and intact plants. The Eu/PTA and Tb/PTA coordination nanoparticles within the *shamrock* and *epipremnum aureum* exhibited distinct morphologies compared to those in previous reports. Multi-color luminescent *shamrocks* were obtained using Eu^{3+}, Tb^{3+}, and their mixture. The nanobiohybrid *shamrocks* could be used to detect Cu^{2+} ions in water. The Ln-CNs-plant nanobiohybrids in this study showcased the capacity to convert living plants into self-powered autosamplers and sensors for environmental and groundwater pollutants. It is well known that plants have evolved complex signaling systems to perceive and rapidly respond to environmental variations. The use of nanotechnology to collect and interpret plant internal responses is of primary importance to enable plants to continuously monitor environmental pollutants in real-time. The species-independent nanotechnology can be applied to any wild-type plants compared with the genetic engineering method. However, the metal ions necessary for plant growth—such as Ca^{2+}—can naturally accumulate in plants and bind to PTA. Phosphate ions in plants also have strong adsorption and chelation to lanthanide ions. These could foreseeably interfere with Ln-CNs formation inside plants. Moreover, the shapes and sizes of Ln-CNs are partially dependent on the biomolecules in plants, and the process is not yet fully understood. Consequently, controllable synthesis of Ln-CNs can be challenging. More *in situ* characterization and separation techniques need to be developed to understand the properties of Ln-CNs grown in plants so that they can be applied more widely. Although only Eu/PTA, Tb/PTA, and Eu/Tb/PTA coordination nanoparticles were synthesized in this study, other nanoparticles and functional materials could theoretically be synthesized in living plants.

Author contributions

Xinnan Wang: conceptualization, investigation, writing-reviewing and editing. Chunyu Zhao: data curation, investigation. Qi Wang: funding acquisition, visualization. Xiaowen Wang: validation, investigation. Tao Chen: investigation.

Xinyue Yang: investigation. Keyi Guo: investigation. Qi Zhou: funding acquisition, writing-reviewing and editing, supervision.

Conflicts of interest

There are no conflicts to declare.

Data availability

Supplementary information: The data supporting this article have been included as part of the SI. See DOI: **https://doi.org/10.1039/d5ra04355g**.

Acknowledgements

This work was supported by the Vice President of Science and Technology Support Program in Henan Province (HNFZ20240007) and the Postdoctoral Fellowship Program of CPSF under Grant Number GZC20232451.

Notes and references

1 S. Yin and C. Tong, *Anal. Chim. Acta*, 2022, **1206**, 339809.
2 Y. M. Wang, Y. Xu, Z. R. Yang, X. Zhang, Y. Hu and R. Yang, *J. Colloid Interface Sci.*, 2021, **598**, 474–482.
3 X. Zhu, X. Wu, J. Liu, L. Zou, B. Ye and G. Li, *Inorg. Chem. Commun.*, 2022, **144**, 109849.
4 X. Wang, K. Gopalsamy, G. Clavier, G. Maurin, B. Ding, A. Tissot and C. Serre, *Chem. Sci.*, 2024, **15**, 6488–6499.
5 L. Han, X. Z. Dong, S. G. Liu, X. H. Wang, Y. Ling, N. B. Li and H. Q. Luo, *Environ. Sci.: Nano*, 2023, **10**, 683–693.
6 M. Runowski, D. Marcinkowski, K. Soler-Carracedo, A. Gorczyński, E. Ewert, P. Woźny and I. R. Martín, *ACS Appl. Mater. Interfaces*, 2023, **15**, 3244–3252.
7 R. Huo, C. Wang, M. Y. Wang, M. Y. Sun, S. Jiang, Y. H. Xing and F. Y. Bai, *Inorg. Chem.*, 2023, **62**, 6661–6673.
8 D. Chen, R. Haldar and C. Wöll, *ACS Appl. Mater. Interfaces*, 2023, **15**, 19665–19671.
9 T. Wiwasuku, A. Chuaephon, U. Habarakada, J. Boonmak, T. Puangmali, F. Kielar, D. J. Harding and S. Youngme, *ACS Sustainable Chem. Eng.*, 2022, **10**, 2761–2771.
10 C. Ji, J. Zhang, R. Fan, Y. Chen, Y. Zhang, T. Sun and Y. Yang, *J. Mater. Chem. C*, 2023, **11**, 2514.
11 H. Yu, Q. Liu, J. Li, Z. Su, X. Li, X. Wang, J. Sun, C. Zhou and X. Hu, *J. Mater. Chem. C*, 2021, **9**, 562–568.
12 W. Wang, C. D. Sessler, X. Wang and J. Liu, *Acc. Chem. Res.*, 2024, **57**, 2013–2026.
13 A. S. Baesso, D. J. Da Silva, A. K. Soares, M. M. D. Silva Paula and P. H. G. de Cademartori, *Ind. Crops Prod.*, 2023, **197**, 116601.
14 N. Zhang, J. Sun, L. Yin, J. Liu and C. Chen, *Adv. Agrochem*, 2023, **2**, 313–323.
15 Y. H. Cheung, K. Ma, M. C. Wasson, X. Wang, K. B. Idrees, T. Islamoglu, J. Mahle, G. W. Peterson, J. H. Xin and O. K. Farha, *Angew. Chem., Int. Ed.*, 2022, **61**, e202202207.
16 E. H. Otal, H. Tanaka, M. L. Kim, J. P. Hinestroza and M. Kimura, *Chem. - Eur. J.*, 2021, **27**, 7376–7382.
17 J. Liang, M. Y. B. Zulkifli, S. Choy, Y. Li, M. Gao, B. Kong, J. Yun and K. Liang, *Environ. Sci. Technol.*, 2020, **54**, 11356–11364.
18 H. A. Castillo-Michel, C. Larue, A. E. Pradas del Real, M. Cotte and G. Sarret, *Plant Physiol. Biochem.*, 2017, **110**, 13–32.
19 M. I. Mattina, W. Lannucci-Berger, C. Musante and J. C. White, *Environ. Pollut.*, 2003, **124**, 375–378.
20 S. Clemens, M. G. Palmgren and U. Krämer, *Trends Plant Sci.*, 2002, **7**, 309–315.
21 K. Liang, R. Ricco, C. M. Doherty, M. J. Styles, S. Bell, N. Kirby, S. Mudie, D. Haylock, A. J. Hill, C. J. Doonan and P. Falcaro, *Nat. Commun.*, 2015, **6**, 7240.
22 J. Hu and Y. Xianyu, *Nano Today*, 2021, **38**, 101143.
23 J. J. Richardson and K. Liang, *Small*, 2018, **14**, 1702958.
24 C. Daiguebonne, C. Blais, K. Bernot and O. Guillou, *Acc. Chem. Res.*, 2025, **58**, 1801–1814.
25 P. R. Donnarumma, C. Copeman, M. Richezzi, J. Sardilli, H. M. Titi and A. J. Howarth, *Cryst. Growth Des.*, 2024, **24**, 1619–1625.
26 C. Blais, T. Morvan, C. Daiguebonne, Y. Suffren, G. Calvez, K. Bernot and O. Guillou, *Inorg. Chem.*, 2023, **62**, 4495–4502.
27 R. Shi, L. Yu, Y. Tian, X. Wang, Z. Sun, B. Qi and F. Luo, *Mater. Chem. Phys.*, 2022, **280**, 125806.
28 X. Z. Dong, Z. Sun, L. Han, Y. Ling, B. L. Li, N. B. Li and H. Q. Luo, *Sens. Actuators, B*, 2022, **372**, 132668.
29 W. T. Wu, X. Chen, Y. T. Jiao, W. T. Fan, Y. L. Liu and W. H. Huang, *Angew. Chem., Int. Ed.*, 2022, **61**, e202115820.
30 J. Krämer, R. Kang, L. M. Grimm, L. D. Cola, P. Picchetti and F. Biedermann, *Chem. Rev.*, 2022, **122**, 3459–3636.
31 S. Y. Kwak, M. H. Wong, T. T. S. Lew, G. Bisker, M. A. Lee, A. Kaplan, J. Dong, A. T. Liu, V. B. Koman, R. Sinclair, C. Hamann and M. S. Strano, *Annu. Rev. Anal. Chem.*, 2017, **10**, 113–140.
32 T. T. S. Lew, V. B. Koman, P. Gordiichuk, M. Park and M. S. Strano, *Adv. Mater. Technol.*, 2020, **5**, 1900657.
33 H. Wei, M. Tang and X. Xu, *Sci. Total Environ.*, 2023, **892**, 164413.
34 B. Hu, L. Jiang, Q. Zheng, C. Luo, D. Zhang, S. Wang, Y. Xie and G. Zhang, *Environ. Int.*, 2021, **155**, 106591.
35 E. E. Sparks and A. Rasmussen, *Plant, Cell Environ.*, 2023, **46**, 2943–2945.
36 M. H. Wong, J. P. Giraldo, S. Y. Kwak, V. B. Koman, R. Sinclair, T. T. S. Lew, G. Bisker, P. Liu and M. S. Strano, *Nat. Mater.*, 2017, **16**, 264–272.
37 T. T. S. Lew, M. Park, J. Cui and M. S. Strano, *Adv. Mater.*, 2021, **33**, 2005683.
38 Y. Cui, Y. Yue, G. Qian and B. Chen, *Chem. Rev.*, 2012, **112**, 1126–1162.
39 Z. Hu, B. J. Deibert and J. Li, *Chem. Soc. Rev.*, 2014, **43**, 5815–5840.